NUCL SCI TECH (2016) 27:131
DOI 10.1007/s41365-016-0138-y

Investigation on symmetry and characteristic properties of the fragmenting source in heavy-ion reactions through reconstructed primary isotope yields

Fang-Fang Duan[1,2] · Xing-Quan Liu[2] · Wei-Ping Lin[2,3] · Ryoichi Wada[4] · Jian-Song Wang[2] · Mei-Rong Huang[4] · Pei-Pei Ren[2,3] · Yan-Yun Yang[2] · Peng Ma[2] · Jun-Bing Ma[2] · Shi-Lun Jin[2] · Zhen Bai[2] · Qi Wang[2]

Received: 20 June 2016 / Revised: 29 June 2016 / Accepted: 11 July 2016 / Published online: 11 October 2016

Abstract In this report, a kinematical focusing technique will be briefly described, and using this technique, the primary hot isotope yields from the multiplicities of evaporated light particles, associated with isotopically identified intermediate mass fragments, are reconstructed. Symmetry energy and characteristic properties of the fragmenting source at the time of the intermediate mass fragment formation are extracted from these reconstructed primary isotope yields using a self-consistent manner. The extracted density-dependent symmetry energy is further compared with those experimentally extracted from other heavy-ion reactions in literatures. A direct connection between the freeze-out concept and transport model simulations in a multifragmenting regime of heavy-ion collisions is also demonstrated quantitatively in the present work.

This work was supported by the Program for the CAS "Light of West China" Program (No. Y601030XB0), the National Basic Research Program of China (No. 2014CB845405) and the National Natural Science Foundation of China (Nos. 11205209 and 11575256).

✉ Xing-Quan Liu
liuxingquan@impcas.ac.cn

✉ Jian-Song Wang
jswang@impcas.ac.cn

[1] School of Physical Science and Technology, Southwest University, Chongqing 400715, China

[2] Institute of Modern Physics, Chinese Academy of Sciences, Lanzhou 730000, China

[3] University of Chinese Academy of Sciences, Beijing 100049, China

[4] Cyclotron Institute, Texas A&M University, College Station, TX 77843, USA

Keywords Symmetry energy · Nuclear temperature · Nuclear density and freeze-out

1 Introduction

In general, the process of heavy-ion induced multifragmentation reactions at the intermediate energy region can be divided into two stages: the early dynamical process, including the compression, the expansion, and the formation of fragments, and the final statistical decay process. The dynamical process is of more focus in last decades, because nuclear matters under critical conditions are generated in this period, and valuable observations are also provided for us to investigate the dynamical mechanism of the nuclear reactions, the density dependence of symmetry energy, and the characteristic properties of the nuclear systems [1–10]. However, in the experiments, the "primary hot" fragments, which are initially generated in the dynamical process, de-excite by a statistical decay process before they are detected as "secondary cold" fragments. This secondary process may significantly alter the information carried by the primary hot fragments, such as the isotope yield distributions among others [11]. Even though the statistical decay process itself is rather well understood and well coded, it is not a trivial task to consider it the data analyses or combine in with a dynamical code.

To eliminate the sequential decay effect, a kinematical focusing technique has been introduced and briefly described in this report. The technique is experimentally employed to evaluate the light particle (LP, including neutrons) multiplicities associated with each isotopically identified intermediate mass fragments (IMFs) for the reaction system ^{64}Zn + ^{112}Sn at 40 MeV/nucleon.

Symmetry energy, temperature, and density at the time of the IMF formation are determined in a self-consistent manner, using the experimentally reconstructed primary hot isotope yields and anti-symmetrized molecular dynamics (AMD) simulations [12–15]. The extracted density-dependent symmetry energy is further compared with those experimentally extracted from other observables in heavy-ion reactions in literatures. Additionally, the freeze-out concept, which is commonly assumed in the statistical models, but not the transport models, is quantitatively connected with the transport model simulations.

2 Method

The kinematical focusing technique utilizes the nature that is in the collisions at intermediate energies, and LPs are generated at different stages of the reaction and from different sources during the evolution of the collisions, but those from the de-excitation of a certain excited isotope are kinematically focused into a cone centered along the isotope direction. To evaluate the LPs associated with an isotopically identified IMF, we first determine the contribution of the uncorrelated particles from other sources. The uncorrelated particles are, on the average, emitted from a variety of sources moving along the beam direction. The kinematically focused correlated particles can be observed as an excess above the uncorrelated spectrum. The excess increases as the opening angle becomes smaller. The average velocity of the correlated particles increases in proportion to the velocity of IMF. Thus, the correlated and uncorrelated particles can be modeled by two moving sources: those are a source moving along the beam direction for the uncorrelated LPs, and the other source moving in the IMF direction for the correlated ones. Then, LP multiplicities associated with an isotopically identified IMF can be extracted by doing integrations for the spectrum of the correlated LPs at different angles. Summing the multiplicities of the given IMF and all the correlated LPs, one can reconstruct the primary hot isotope multiplicity. More details about the kinematical focusing technique and the reconstruction of the primary hot fragments can be found in Ref. [16]. The isotope multiplicity distributions of the experimentally reconstructed primary hot isotope ($Z = 3 - 14$) for the reaction system ^{64}Zn + ^{112}Sn at 40 MeV/nucleon are shown in Fig. 1, comparing with those from the direct experimental measurement and the AMD simulations.

The symmetry energy and the temperature and density of the fragmenting source are extracted from the experimentally reconstructed primary hot isotope yields using a self-consistent manner [17–20], with the help of AMD simulations. The brief processes of the self-consistent technique are

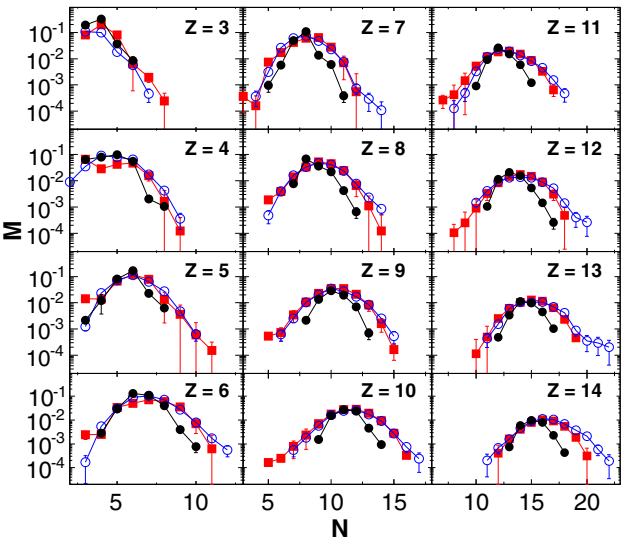

Fig. 1 (Color online) Isotope multiplicity distributions of experimental cold fragments (*dots*), reconstructed hot fragments (*closed squares*), and AMD primary hot fragments (*circles*) as a function of fragments mass number, *A*, for a given charge, *Z*, which is indicated in the figure (cited from Ref. [17]). In the AMD simulations, g0AS interaction is used

as follows: (a) optimize symmetry energy relative to temperature, $a_{\rm sym}/T$, from the isotope yields of the experimentally reconstructed primary fragments and AMD simulations with three different types of density dependence of symmetry energies in the frame work of modified Fisher model (MFM) [21]; (b) extract the density, ρ, by comparing with the resultant $a_{\rm sym}/T$ values from the AMD simulations with different density dependence of the symmetry energy; (c) extract the $a_{\rm sym}$ values from the extracted ρ value and the comparison between the $a_{\rm sym}/T$ values from the isotope yields of the experimentally reconstructed and AMD-simulated primary fragments; and (d) calculate the temperature, T, from the ratio of $a_{\rm sym}$ to $a_{\rm sym}/T$. More detailed description of the self-consistent manner is given in Refs. [17–19]. The symmetry energy and the temperature and density at the time of the IMF formation are evaluated as $a_{\rm sym} = 23.1 \pm 0.6$ MeV, $\rho/\rho_0 = 0.65 \pm 0.02$, and $T = 5.0 \pm 0.4$ MeV, respectively, for the fragmenting system experimentally observed in the reaction studied. It should be emphasized that the temperature obtained in this work is much higher than those experimentally extracted from secondary cold IMFs [22–24].

3 Results and discussion

In Fig. 2, the density-dependent symmetry energy obtained in our present work and other experimentally extracted results from various observables are summarized.

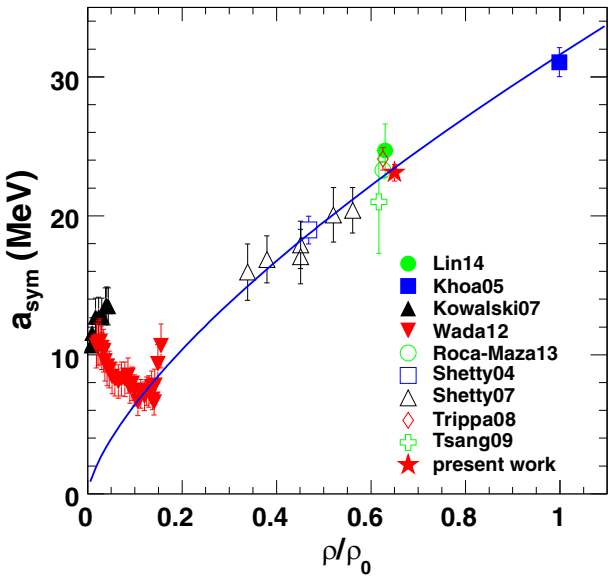

Fig. 2 (Color online) Summary of the density-dependent symmetry energy obtained in the present and previous studies. The line is the fit of the existing data points at $0.1 < \rho/\rho_0 \leq 1.0$ with $a_{sym}(\rho/\rho_0) = a_{sym}^{\rho=\rho_0} \cdot (\rho/\rho_0)^{\gamma}$

All of the data points cited are the results which are determined based on the nuclear reactions [7, 18, 25–31]. One can observe two groups of data points: those are $\rho/\rho_0 \lesssim 0.1$ and $0.1 \lesssim \rho/\rho_0 \leq 1.0$, respectively. For lower densities ($\rho/\rho_0 \lesssim 0.1$), the significant deviation from others can be attributed to the formation of clusters at low densities [27, 32]. For $0.1 \lesssim \rho/\rho_0 \leq 1.0$, the existing data points are consistent with each other within the errors and distribute along a line as a function of density. Under the assumption of mean field, the density-dependent symmetry energy is phenomenologically parameterized as a power function, $a_{\mathrm{sym}}(\rho/\rho_0) = a_{\mathrm{sym}}^{\rho=\rho_0} \cdot (\rho/\rho_0)^{\gamma}$, where $a_{\mathrm{sym}}^{\rho=\rho_0}$ is the symmetry energy value at the saturation density and γ is a parameter for describing the "stiffness" of the density-dependent symmetry energy. Fitting the data points at $0.1 < \rho/\rho_0 \leq 1.0$ with this power relation, one can obtain $a_{\mathrm{sym}}(\rho/\rho_0) = 31.6 \cdot (\rho/\rho_0)^{0.69}$, which suggests a stiff, but softer than linear form of symmetry energy at subsaturation densities. This result is also more or less consistent with those from other parallel theoretical approaches [33, 34].

To model the multifragmentation process, a number of different models have been developed in two distinct scenarios at the intermediate energy region. One is based on a statistical multifragmentation under thermal and chemical equilibriums at a freeze-out volume, and the other one is based on a transport theory, in which nucleon propagation in a mean field and nucleon–nucleon collisions under Pauli blocking are two main ingredients. No freeze-out concept is assumed within transport models. To investigate the freeze-out concept in transport models, AMD events are generated for central collisions ($b = 0$ fm) of ^{40}Ca + ^{40}Ca at 35, 50, 80, 100, 140, and 300 MeV/nucleon. The density and temperature of the fragmenting sources from these reaction systems have been extracted using the self-consistent method mentioned above.

The extracted density and temperature values in the incident energy range studied here are summarized in Fig. 3. The extracted density values (filled circles) are plotted together with the maximum density created during the collisions (open circles) in (a). The maximum density values are calculated at the origin of the center of mass system and normalized by the density of the initial nuclei at $t = 0$ fm/c. They increase monotonically from $\rho/\rho_0 \sim 1.3$ at 35 MeV/nucleon to ~ 1.8 at 300 MeV/nucleon. On the contrary, the extracted density values for the fragmenting source distribute at $\rho/\rho_0 \sim 0.65$–0.7. The extracted temperature values (red dots connected by lines) in (b) show also more or less a constant distribution, and T_0 values of 5.9–6.5 MeV are obtained. These flat distributions of the extracted density and temperature values indicate that IMFs are in average formed at a later stage when the hot

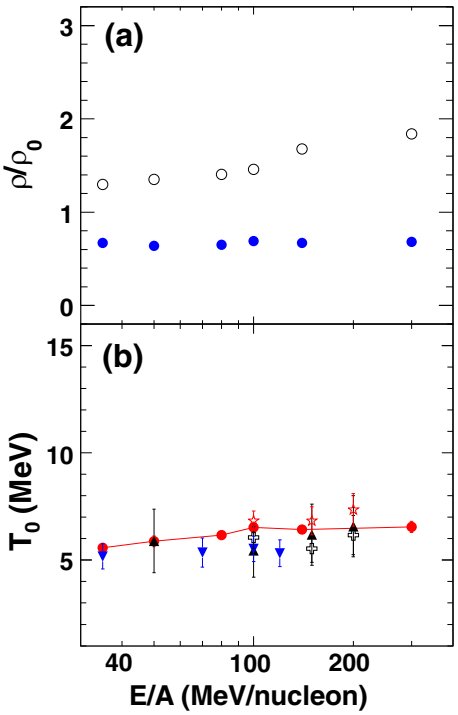

Fig. 3 (Color online) **a** Extracted ρ/ρ_0 values (*filled circles*) and the maximum ρ/ρ_0 values (*open circles*) as a function of the incident energy **b** extracted T_0 values from the final rounds (*red dots* connected by *lines*). *Filled triangles* (*black*) and *filled inverted triangles* (*blue*) are taken from Serfling et al. [36] and Xi et al. [35], respectively. These data points are corrected for the sequential decay effect by multiplying a factor of 1.2 [36]. *Open cross* and starts are the results from CLi and CC thermometer in Ref. [37]

nuclear matter reaches at a "freeze-out" volume by the expansion.

MFM assumes a single temperature of the fragmenting system, based on the thermal and chemical equilibrium at the time of IMF production. In AMD simulation, the IMF production shows significant variation in time and space on an event-by-event basis. Therefore, the temperature extracted in the present work is an average temperature in time and among IMF species. There is also no reason to assume all particles are produced at a single temperature. Therefore, one has to be cautious to compare our results to those extracted by different thermometers with different particles involved. Here, we compare our results with those extracted by thermometers mainly using IMFs in the published works. In Fig. 3b, our results are presented by filled red circles connected with lines. Filled black and blue inverted triangles are those from the excited-state populations of particle-unstable resonances of ^{8}Be in the central ^{197}Au on ^{197}Au collisions at 50–200 MeV/nucleon [36] and the central and semi-central collisions of ^{86}Kr on ^{93}Nb at 35–120 MeV/nucleon [35], respectively. These values show similar to those from our present results after correcting the sequential decay effects in their results [36], even though they have larger error bars. The open symbols in Fig. 3b are from different double isotope thermometers from the central ^{197}Au on ^{197}Au collisions [37], and the QSM correction has been applied for the sequential feeding as described in the reference. Both of the temperature values from carbon–lithium isotope ratio (CLi, black crosses) and carbon–carbon isotope ratio (CC, red stars) show more or less constant values ($\sim$6 MeV) independent on the incident energies in (b).

4 Summary

A kinematical focusing technique is introduced to reconstruct the primary hot isotope yields from the experimentally measured secondary cold isotope yields. This kinematical focusing technique is applied to experimentally reconstruct the yields of primary hot fragments for multifragmentation events in the reaction system ^{64}Zn + ^{112}Sn at 40 MeV/nucleon. Using the reconstructed hot isotope yields, the AMD simulations with the Gogny interaction with three different density-dependent symmetry energy terms, and a self-consistent approach based on the modified Fisher model, symmetry energy and characteristic properties of the fragmenting source at the time of the IMF formation are extracted as $a_{\rm sym} = 23.1 \pm 0.6$ MeV, $\rho/\rho_0 = 0.65 \pm 0.02$, and $T = 5.0 \pm 0.4$ MeV, respectively. The extracted values are compared with those extracted from other observables in heavy-ion reactions. From the fit of the existing data points within the mean field theory, a stiff, but softer than linear form of symmetry energy at subsaturation densities, is suggested.

Using the above self-consistent method, the density and temperature of the fragmenting system for the IMF production are studied using the AMD-simulated ^{40}Ca+^{40}Ca events in the incident energy range from 35 to 300 MeV/nucleon. The extracted density and temperature values are, respectively, $\rho/\rho_0 \sim 0.65$–0.7 and $T_0 \sim 5.9$–6.5 MeV under a thermal and chemical equilibrium assumption in this incident energy range. These rather constant values as a function of the incident energy indicate that there is a "freeze-out" volume for the IMF production in the heavy-ion reactions at intermediate energies, which is commonly used in the statistical multifragmentation model as the basic assumption.

References

1. B.A. Li, L.W. Chen, C.M. Ko, Recent progress and new challenges in isospin physics with heavy-ion reactions. Phys. Rep. **464**, 113 (2008). doi:10.1016/j.physrep.2008.04.005
2. M.B. Tsang, W.A. Friedman, C.K. Gelbke et al., Isotopic scaling in nuclear reactions. Phys. Rev. Lett. **86**, 5023 (2001). doi:10.1103/PhysRevLett.86.5023
3. M.B. Tsang, T.X. Liu, L. Shi et al., Isospin diffusion and the nuclear symmetry energy in heavy ion reactions. Phys. Rev. Lett. **92**, 062701 (2004). doi:10.1103/PhysRevLett.92.062701
4. M.A. Famiano, T. Liu, W.G. Lynch et al., Neutron and Proton transverse emission ratio measurements and the density dependence of the asymmetry term of the nuclear equation of state. Phys. Rev. Lett. **97**, 052701 (2006). doi:10.1103/PhysRevLett.97.052701
5. T. Li, U. Garg, Y. Liu et al., Isotopic dependence of the giant monopole resonance in the even-A $^{112-124}$Sn isotopes and the asymmetry term in nuclear incompressibility. Phys. Rev. Lett. **99**, 162503 (2007). doi:10.1103/PhysRevLett.99.162503
6. A. Klimkiewicz, N. Paar, P. Adrich et al., Nuclear symmetry energy and neutron skins derived from pygmy dipole resonances. Phys. Rev. C **76**, 051603 (2007). doi:10.1103/PhysRevC.76.051603
7. L. Trippa, G. Colo, E. Vigezzi, Giant dipole resonance as a quantitative constraint on the symmetry energy. Phys. Rev. C **77**, 061304 (2008). doi:10.1103/PhysRevC.77.061304
8. Z. Kohley, M. Colonna, A. Bonasera et al., Sensitivity of intermediate mass fragment flows to the symmetry energy. Phys. Rev. C **85**, 064605 (2012). doi:10.1103/PhysRevC.85.064605
9. H.S. Xu, M.B. Tsang, T.X. Liu et al., Isospin fractionation in nuclear multifragmentation. Phys. Rev. Lett. **85**, 716 (2000). doi:10.1103/PhysRevLett.85.716
10. M.B. Tsang, C.K. Gelbke, X.D. Liu et al., Isoscaling in statistical models. Phys. Rev. C **64**, 054615 (2001). doi:10.1103/PhysRevC.64.054615
11. M. Huang, Z. Chen, S. Kowalski et al., Isobaric yield ratios and the symmetry energy in heavy-ion reactions near the Fermi energy. Phys. Rev. C **81**, 044620 (2010). doi:10.1103/PhysRevC.81.044620
12. A. Ono, H. Horiuchi, Antisymmetrized molecular dynamics of wave packets with stochastic incorporation of the Vlasov

equation. Phys. Rev. C **53**, 2958 (1996). doi:10.1103/PhysRevC.53.2958
13. A. Ono, Antisymmetrized molecular dynamics with quantum branching processes for collisions of heavy nuclei. Phys. Rev. C **59**, 853 (1999). doi:10.1103/PhysRevC.59.853
14. A. Ono, S. Hudan, A. Chbihi et al., Compatibility of localized wave packets and unrestricted single particle dynamics for cluster formation in nuclear collisions. Phys. Rev. C **66**, 014603 (2002). doi:10.1103/PhysRevC.66.014603
15. A. Ono, H. Horiuchi, Antisymmetrized molecular dynamics for heavy ion collisions. Prog. Part. Nucl. Phys. **53**, 501 (2004). doi:10.1016/j.ppnp.2004.05.002
16. M.R.D. Rodrigues, W. Lin, X. Liu et al., Experimental reconstruction of excitation energies of primary hot isotopes in heavy ion collisions near the Fermi energy. Phys. Rev. C **88**, 034605 (2013). doi:10.1103/PhysRevC.88.034605
17. X. Liu, W. Lin, R. Wada et al., Reconstructed primary fragments and symmetry energy, temperature and density of the fragmenting source in ^{64}Zn + ^{112}Sn source at 40 MeV/nucleon. Nucl. Phys. A **933**, 290 (2014). doi:10.1016/j.nuclphysa.2014.09.077
18. W. Lin, X. Liu, M.R.D. Rodrigues et al., Novel determination of density, temperature, and symmetry energy for nuclear multifragmentation through primary fragment-yield reconstruction. Phys. Rev. C **89**, 021601(R) (2014). doi:10.1103/PhysRevC.89.021601
19. X. Liu, W. Lin, R. Wada et al., Primary isotope yields and characteristic properties of the fragmenting source in heavy-ion reactions near the Fermi energy. Phys. Rev. C **90**, 014605 (2014). doi:10.1103/PhysRevC.90.014605
20. X. Liu, M. Huang, R. Wada et al., Symmetry energy extraction from primary fragments in intermediate heavy-ion collisions. Nucl. Sci. Tech. **26**, S20508 (2015). doi:10.13538/j.1001-8042/nst.26.S20508
21. M.E. Fisher, The theory of equilibrium critical phenomena. Rep. Prog. Phys. **30**, 615 (1967). doi:10.1088/0034-4885/30/2/306
22. C.W. Ma, J. Pu, Y.G. Ma et al., Temperature determined by isobaric yield ratios in heavy-ion collisions. Phys. Rev. C **86**, 054611 (2012). doi:10.1103/PhysRevC.86.054611
23. C.W. Ma, X.L. Zhao, J. Pu et al., Temperature determined by isobaric yield ratios in a grand-canonical ensemble theory. Phys. Rev. C **88**, 014609 (2013). doi:10.1103/PhysRevC.88.014609
24. C.W. Ma, T.T. Ding, C.Y. Qiao et al., Improved thermometer for intermediate-mass fragments in heavy-ion collisions with isobaric yield ratio difference. Phys. Rev. C **92**, 064601 (2015). doi:10.1103/PhysRevC.92.064601
25. D.T. Khoa, H.S. Than, Isospin dependence of ^{6}He+p optical potential and the symmetry energy. Phys. Rev. C **71**, 044601 (2005). doi:10.1103/PhysRevC.71.044601
26. S. Kowalski, J.B. Natowitz, S. Shlomo et al., Experimental determination of the symmetry energy of a low density nuclear gas. Phys. Rev. C **75**, 014601 (2007). doi:10.1103/PhysRevC.75.014601
27. R. Wada, K. Hagel, L. Qin et al., Nuclear matter symmetry energy at $0.03 < \rho/\rho_0 < 0.2$. Phys. Rev. C **85**, 064618 (2012). doi:10.1103/PhysRevC.85.064618
28. X. Roca-Maza, M. Brenna, B.K. Agrawal et al., Giant quadrupole resonances in ^{208}Pb, the nuclear symmetry energy, and the neutron skin thickness. Phys. Rev. C **87**, 034301 (2013). doi:10.1103/PhysRevC.87.034301
29. D.V. Shetty, S.J. Yennello, A.S. Botvina et al., Symmetry energy and the isospin dependent equation of state. Phys. Rev. C **70**, 011601(R) (2004). doi:10.1103/PhysRevC.70.011601
30. D.V. Shetty, S.J. Yennello, G.A. Souliotis, Density dependence of the symmetry energy and the nuclear equation of state: a dynamical and statistical model perspective. Phys. Rev. C **76**, 024606 (2007). doi:10.1103/PhysRevC.76.024606
31. M.B. Tsang, Y.X. Zhang, P. Danielewicz et al., Constraints on the density dependence of the symmetry energy. Phys. Rev. Lett. **102**, 122701 (2009). doi:10.1103/PhysRevLett.102.122701
32. J.B. Natowitz, G. Ropke, S. Typel et al., Symmetry energy of dilute warm nuclear matter. Phys. Rev. Lett. **104**, 202501 (2010). doi:10.1103/PhysRevLett.104.202501
33. K.S. Vinayak, S. Kumar, On the role of density-dependent symmetry energy and momentum dependent interactions in multi-fragmentation. Phys. Part. Nucl. Lett. **9**, 583 (2012). doi:10.1134/S1547477112080109
34. K.S. Vinayak, S. Kumar, Effect of density-dependent symmetry energy on nuclear stopping. J. Phys. G Nucl. Part. Phys. **39**, 095105 (2012). doi:10.1088/0954-3899/39/9/095105
35. H.F. Xi, G.J. Kunde, O. Bjarki et al., Dynamical emission and isotope thermometry. Phys. Rev. C **58**, 2636(R) (1998). doi:10.1103/PhysRevC.58.R2636
36. V. Serfling, C. Schwarz, R. Bassini et al., Temperatures of exploding nuclei. Phys. Rev. Lett. C **80**, 3928 (1998). doi:10.1103/PhysRevLett.80.3928
37. W. Trautmann, R. Bassini, M. Begemann-Blaich et al., Thermal and chemical freeze-out in spectator fragmentation. Phys. Rev. C **76**, 064606 (2007). doi:10.1103/PhysRevC.76.064606